Electric Power Systems Research 173 (2019) 281–290

Contents lists available at ScienceDirect

Electric Power Systems Research

journal homepage: www.elsevier.com/locate/epsr

Optimal placement and sizing of multiple active power filters in radial distribution system using grey wolf optimizer in presence of nonlinear distributed generation

Ashokkumar Lakum*, Vasundhara Mahajan

Electrical Engineering Department, Sardar Vallabhbhai National Institute of Technology, Surat, 395007, India

ARTICLE INFO

Keywords:
Active power filter (APF)
Distributed generation (DG)
Grey wolf optimizer (GWO)
Radial distribution system (RDS)

ABSTRACT

Excessive utilization of distributed generation (DG) leads to power quality issues in the radial distribution system (RDS). The harmonic level exceeds the IEEE-519 standard limits if DG penetration level extends. In this paper, the impact of DG penetration on the optimal placement and sizing (OPAS) of active power filter (APF) is discussed. The new nonlinear load position based APF current injection (NLPCI) technique is proposed to locate the feasible buses for the placement of APF in presence of nonlinear load only as well as in presence of DG also. Here, the grey wolf optimizer (GWO) is used to recognize the optimal size of APF. The result shows that the size of APF required with inclusion of nonlinear load and DG is bigger as compared to that with nonlinear load only. The GWO outcomes are compared with the results of particle swarm optimization (PSO) and harmony search (HS). The result shows that penetration of DG affects the placement and size of APF, and GWO gives significant outcomes compared to PSO and HS.

1. Introduction

Distributed generation (DG) is a miniature-scale scattered source of electric power located near to the loads being serviced. Several DG technologies are in practice such as wind turbines, photovoltaic (PV) cells, small hydro, biomass, fuel cells, micro-turbines, and others [1]. DGs have been extensively functioned in the distribution systems considering procedural advantages for the power grids such as power loss minimization, improvement of voltage profile and system security, reliability enrichment, and energy efficiency augmentation [2,3]. Moreover, energy crunch caused due to the deficiency of the conventional energy supplies such as natural gas and petroleum, and the extended interests to global warming and climate change have pushed all the stakeholders together with administrators of distribution companies to concentrate on the full employment of the DG technologies with the use of environmentally favorable renewable energy resources [4]. The investment in the DG technologies may serve a genuine possibility to adhere the load progression by utilizing cost-effective, low-carbon, high-efficiency capability augmentation alternatives.

In the past, the grid-connected DGs were inadequate and produced a notable disturbance in the distribution systems. Currently, with the remarkable progress in systems combination with dispersed generation units, this state is shifting, and the thought of 100% penetration is getting alike. However, redundant inclusion or improper DG sizes may originate disagreeable results in the electrical systems such as power quality, energy efficiency, and protection issues [5,6]. Among the DGs, PV system is treated as a green technology due to its advantages as it is noise-free, easy to install, no emission and requires very less maintenance. Its future growth in the power system is estimated very high due to advancement in technology and reduction in cost. However, PV integration into the power system have drawbacks along with its advantages. Pulse width modulator (PWM) is used to interface a PV system with a distributed system. PWM is one of the primary sources of harmonics. When DG injects the harmonics into the system, it is considered as nonlinear DG (NLDG) [7–10].

Optimal planning, sizing, and placement of DG units in the distribution networks are well-thought-out in many works. In the available literature, various strategy purposes are estimated for the optimal planning problem of DG units such as to reduce system power losses, reactive power control, voltage profile improvement, system security improvement and reliability enhancement, and exhaust the possibilities of the DG penetration [11].

In recent years, DG with its harmonic distortion effect in radial distribution system (RDS) has been discussed [12–16]. The excessive or inappropriate use of DG in RDS creates power quality problem; notably increases the harmonic level beyond the IEEE-519 standards which is

* Corresponding author.
E-mail addresses: aclakum@gmail.com (A. Lakum), vasu.daygood@gmail.com (V. Mahajan).

https://doi.org/10.1016/j.epsr.2019.04.001
Received 12 September 2018; Received in revised form 5 March 2019; Accepted 1 April 2019
Available online 09 May 2019
0378-7796/

5% for the total harmonic distortion in voltage (THDv) and 3% for the individual harmonic distortion in voltage (IHDv) [17]. Reduction in harmonics is desirable when talking about the DG. The individual harmonic distortion of a particular DG may be below the IEEE limits, but when they are connected in RDS; their cumulative effects increase the harmonic level beyond the IEEE standards. Maintaining the THDv below 5% is compulsory hence the filters are required to reduce the harmonics in RDS.

Passive filters (PF) are typically used for the mitigation of harmonics, but they suffer from the disadvantages such as fixed or step compensation, larger size and the possibility of resonance with line impedance. These disadvantages are overcome by the use of Active Power Filters (APFs) apparently having a more considerable cost than the PF [18]. In light of the above discussion, to cancel out the harmonic distortion, APF should be implemented at all the nonlinear loads and NLDG buses. Thus, THDv at all the buses can be made nearly zero. However, to apply APFs at all the buses is too costly.

Moreover, THDv need not to be zero, as IEEE standards are allowing it up to 5%. So, optimization of APFs is utmost required. Hence, the harmonics injected by the NLDG is an essential factor to be considered for the size of APF to mitigate harmonics up to allowable limits. Moreover, it also affects the placement of APF. Therefore, for the realistic assessment of an interconnected system with power flow, it is essential to incorporate NLDGs in optimal placement and sizing (OPAS) of APF.

The various indices considering power loss, voltage, current, short circuit, DG capacity, financial and environmental criteria have been used to find the OPAS of DG [11,19–22]. The minimization of losses and maximization of DG capacity is analyzed in Ref. [19]. In Ref. [20], a fast clustering technique has been employed to connect the DG. Various indices considering node, DG, external suppliers, energy storage system, and vehicle to grid have been used for cost allocation modeling of distribution network with high penetration of DG in Ref. [21]. In Ref. [22], voltage stability index has been proposed with novel comparison of power loss sensitivity and power stability index. It has been stated that, proposed method is providing better planning and management for DG in RDS. In Ref. [23], OPAS of DG has been done using three indices- active power loss index, line loading index, and voltage deviation index. In Ref. [24], unified bus performance index has been adopted for techno economic assessment of power quality mitigation solutions in networks integrated with DG. Ref. [25] has been provided the systematic and extensive overview of hosting capacity research with addressing several performance indices like power system harmonics, over voltage, thermal over loading, hosting capacity co-efficient, feeder reinforcement, and harmonic penetration ratio; related to DG.

Moreover, researchers have discussed various optimization methods for finding OPAS of APF such as genetic algorithm (GA) [26], particle swarm optimization (PSO) and its modified versions [27–30], ant colony optimizer (ACO) [31], harmony search (HS) algorithm [32–34], firefly algorithm (FA) [35]. GA has been used for finding the optimal allocation and size of AFP in Ref. [26] with minimizing the harmonics. Three scenarios- five buses, ten buses, and all buses in IEEE-18 bus system for bus selection have been considered in Ref. [34]. The power quality in smart grid network has been improved by optimal siting, sizing and operation of custom power devices with active power line conditioner in Ref. [36]. In the research papers listed above mostly the optimization algorithm takes the entire burden of finding the buses for placement as well as size of APF.

As stated above various indices are incorporated for OPAS of DG. However, less attention is paid to the techniques used for finding the feasible buses for APF placement, in the available literature. In this paper, the nonlinear load position based APF current injection (NLPCI) technique is proposed to find the feasible buses for APF placement in presence of NLDG. According to the position of nonlinear loads the possible placement of APF is considered. When only nonlinear load is considered, the current rating of APF is same as that of nonlinear load but when nonlinear load plus NLDG are considered together, APF current rating is same as that of nonlinear load and NLDG. Using this technique, the feasibility of buses for placement of APF is found. The output consists of the feasible buses, which are fulfilling the constraints as well as unfeasible buses which are not fulfilled the constraints with THDv at all buses.

The main advantages of NLPCI are: (1) Simple (2) It gives accurate result (3) It finds the feasible buses for APF placement, thus it reduces the search space resulted in minimization of the computational burden on the optimization algorithm. The novelty of the paper includes: (1) Authors have proposed a novel NLPCI technique to find the feasible buses for the placement of APF in presence of NLDG. (2) Using NLPCI, optimization algorithm used for finding the optimal size of APF at feasible buses only instead of considering all buses of RDS.

In the literature, various optimization techniques and its variants have been proposed for the OPAS of multiple APFs such as GA, PSO, ACO, HS algorithm, FA, and cuckoo search algorithm. All of the above techniques require tuning of their algorithm-specific control parameters except the common controlling parameters (population size and number of generations). Improper tuning of these parameters gives irrelevant result, leads to weak convergence, and possibility to be trapped in local optima. Proper tuning of these parameters is a separate optimization problem. Moreover, no free lunch (NFL) theorem [37] logically proves that no algorithm can solve all optimization problems and hence encourages researchers to use different optimization algorithms. To the best of Author's knowledge, the grey wolf optimizer (GWO) is not used for OPAS of APF in the presence of NLDG. GWO entertains less burden of tuning of algorithm specific parameters compared to PSO and HS. Also the GWO was the 1st most downloaded and the 2nd most cited article in Advances in Engineering Software Articles (Elsevier- Journal) in 2015. Above all things motivated authors to use GWO for the OPAS of APF problem.

To the best of authors' knowledge over the published research papers in the field of OPAS of APF considering NLDG, the main contributions of this paper is:

- The NLPCI technique is proposed to find the feasible buses for APF placement. NLPCI technique which is shown in the paper is completely new technique. It finds the feasible buses for APF placement.
- OPAS of APF for harmonic reduction as per the IEEE 519 standards limits in RDS with integration of NLDG is analyzed.
- The GWO, PSO and HS are used for finding the size of APF in the presence of nonlinear loads and NLDGs. Extensive computational tests concerning best value, average value, worst value and statistical tests are carried out for finding the size of APF.
- It is analyzed that the requirement of APF is more when the NLDG is penetrated in the RDS compared to without NLDG. It is also proved that GWO performs better compared to PSO and HS in computational tests as it gives minimum value of APF current in both cases.

In the next part of the paper, the problem formulation including the implementation of GWO for OPAS of APF is represented. Finally, simulation results are analyzed and discussed followed by the conclusion.

2. Problem formulation

Mathematical modeling of the RDS with the NLDGs, nonlinear loads and harmonic filters is shown in Fig. 1. The process to model the individual element of the system and harmonic load flow with GWO is given below.

2.1. Modeling of RDS

The RDS is represented as branch impedance $Z_{a,b}$ that is given as,

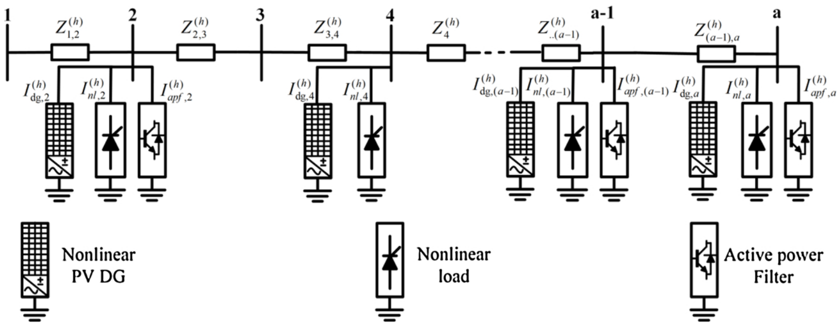

Fig. 1. RDS with nonlinear loads, NLDGs and APFs.

$$Z_{a,b} = R_{a,b} + jX_{L,a,b} \tag{1}$$

As RDS contain NLDGs and nonlinear loads, the branch impedance $Z_{a,b}^{(h)}$ with harmonics is written as,

$$Z_{a,b}^{(h)} = R_{a,b} + jX_{L,a,b}^{(h)} \tag{2}$$

$$X_{La,b}^{(h)} = \omega_h L_{a,b} \tag{3}$$

$$\omega_h = 2\pi f_h \tag{4}$$

Here h represents the order of harmonics, a and b are bus numbers, $R_{a,b}$ is resistance of branch ab, $L_{a,b}$ is inductance of branch ab, ω_h is the angular frequency of the harmonic current, and f_h is the harmonic frequency of current.

2.2. Modeling of nonlinear load

The nonlinear loads are modeled as harmonic current injection source [27,33], and their rms value is given as,

$$I_{nl,a}^{(h)} = I_{nl,a,r}^{(h)} + jI_{nl,a,im}^{(h)} \tag{5}$$

$$I_{nl,a} = \sqrt{\sum_{h=2}^{H} (I_{nl,a,r}^{2(h)} + I_{nl,a,im}^{2(h)})} \tag{6}$$

Here $I_{nl,r}^{(h)}$ and $I_{nl,im}^{(h)}$ are the real and imaginary parts of the load current, $I_{nl,a}$ is the rms value for the nonlinear load current at bus a and H is the highest order of harmonics.

2.3. Modeling of APF

The APF is modeled as a current source [27,33]. It is set of current sources which inject different order of harmonics at a point of common coupling (PCC) according to the current of nonlinear load and NLDG. The phasor model of APF is given as

$$I_{apf,a}^{(h)} = I_{apf,a,r}^{(h)} + jI_{apf,a,im}^{(h)} \tag{7}$$

$$I_{apf,a} = \sqrt{\sum_{h=2}^{H} (I_{apf,a,r}^{2(h)} + I_{apf,a,im}^{2(h)})} \tag{8}$$

where $I_{apf,r}^{(h)}$ is the real and $I_{apf,im}^{(h)}$ is the imaginary part of APF current, $I_{apf,a}$ is the rms value of current of APF at bus a. Here APF is used for harmonic mitigation and therefore resonance is neglected.

2.4. Modeling of DG

The DG injects the nonlinear current into the system. It is modeled as a current source [12,13]. From the power rating of the DG, the fundamental current is calculated [12]. Now, according to the harmonic spectrum of the NLDG harmonic current is calculated as

$$I_{dg,a}^{(h)} = K_{dg} I_{dg,a} \tag{9}$$

where $I_{dg,a}^{(h)}$ is the harmonic current of DG, K_{dg} is the percentage of harmonic current as per the harmonic spectrum of DG, $I_{dg,a}$ is the fundamental current of DG.

2.5. Harmonic load flow

In this paper, bus injection to branch current (BIBC) and branch current to the bus voltage (BCBV) matrices based harmonic load flow technique is used [38]. It is coupled with GWO, PSO, and HS for OPAS of multiple APFs.

The THD_V at bus a is given as,

$$THDv_{,a} = \frac{\sqrt{\sum_{h=2}^{H} (IHDv_{,a})^2}}{V_{f,a}^1} \tag{10}$$

where $V_{f,a}^1$ is fundamental frequency voltage at bus a.

This harmonic distortion calculation is appropriated for identifying the critical buses where the IEEE standard limits are violated. The identification of the critical buses will help in deciding the strategy to mitigate the harmonics by installing harmonic filters. Optimization determines the rating and the number of these filters.

2.6. Optimization process

The optimization method involves the objective function (maximize or minimize), parameters (variables) and constraints. The optimization algorithm optimizes the objective function by optimizing the variables. The variables are the principal inputs to the system and may be subjected to the constraints if needed. The constraints define the limitations applied to the system and feasibility of the value of the objective function in the search space. As mentioned earlier, the identification of bus number, location, and size of APFs is to be optimized to minimize the cost. For the stated problem, it is essential to minimize the APF current as the cost of APF increases with the increment in its current rating. Hence, this is a nonlinear optimization problem with constraints, and the determination variable is the measure of the current of APF. The objective function (OF_{Iflt}) is formed in the form of rms value of the current of APF subjected to three inequality constraints as,

$$OF_{Iflt} = \min \sum_{j=1}^{Nf} I_{apf,j} + DP \tag{11}$$

Subjected to constraints: $THDv \le 5\%$, $IHDv \le 3\%$, and $I_{apf} \le I_{apf,max}$ with $I_{apf,max}$ as the maximum APF current, DP is dynamic penalty.

Generally, the penalty functions are divided into two classes: (1) static penalty- it is a function of the degree of violation of constraints; and (2) dynamic penalty-this penalty is a function of iteration number in addition to the degree of violation of constraints [39]. Here, dynamic penalty function (DP) is used for constraints handling and added to the objective function to discard the infeasible solutions. The amount of penalty is adjusted during the optimization process. The penalty is zero if the constraints are satisfied and high if the constraints are not fulfilled. The penalty increases with increase in violation limits. It has the characteristic of allowing highly infeasible solutions early in search space. The continuous increase in the penalty forced ultimately shifts the final solutions to the feasible region.

Here, I_{apf} depends on the resultant nonlinear current at PCC. Resultant nonlinear current ($I_{nl,dg}$) is vector summation of a nonlinear current of loads and DGs. The summation of harmonic currents depends on the phase angle, if an angle is 180°, the lowest distortion is observed, while for zero phase angle it is worst. Hence, it is cleared that when harmonic currents are in phase, the worst distortion will occur. Here, it is assumed that the PV DG generates only active power [12].

$$I_{nl,dg} = I_{nl} + I_{dg} \tag{12}$$

$$I_{apf} = k(I_{nl,dg}) \tag{13}$$

where, k is proportionate of resultant nonlinear current, which is required to satisfy the constraints.

The IEEE standard 519 dictates the first two constraints, and the third constraint is regulated by the nonlinear load current plus NLDG current.

To solve the OPAS of multiple APFs, NLPCI, GWO, PSO, and HS algorithms are implemented, and GWO is described in the next section.

2.7. GWO for OPAS of APFs considering nonlinear loads and DGs

The GWO is based upon swarm intelligence, and it was proposed by Mirjalili et al. [40]. It is widely used for optimization problems [41,42]. The benefit of GWO is that it analyzes the system as a black box as shown in Fig. 2. It provides the variables to the system as input and observes the output. Here the input is current of APFs and output is the value of objective function. The GWO then iteratively modifies the inputs of the system according to the feedbacks (output) received so far until the attainment of end criteria.

The objective function determined for each position of the grey wolf is mapped into the harmonic load flow data as the current of APF at a bus. The smallest value of fitness function (best fitness) is saved as the alpha score, and the corresponding variables are as an alpha position. Similarly, second and third best fitness and positions are saved in the form of beta and delta respectively. Then, the hunt agents refresh their positions to best fit. This process extends to the highest quantity of iterations. The flowchart of the algorithm is shown in Fig. 3 and the steps of implementation are as follows:

Step-(1) Arrange the parameters: In this step, number of runs (N_{run}), number of search agents (N_{sa}) and maximum number of iterations (T) are set.

Step-(2) Initialization: Initialize the scores and positions of alpha, beta, and delta. The location of grey wolves is randomly produced by the algorithm in the initial iteration, and then it is refreshed for every iteration. The position matrix at t^{th} iteration is as,

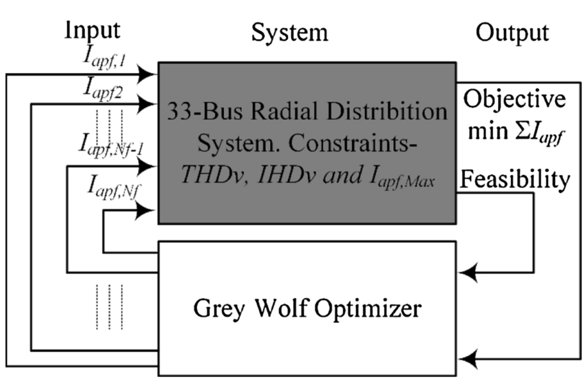

Fig. 2. Block diagram of GWO for optimal sizing of multiple APFs in RDS.

$$\vec{I}_{apf,pos}(t) = \begin{bmatrix} \vec{I}^{1}_{apf,1} & \vec{I}^{1}_{apf,2} & \cdots & \cdots & \vec{I}^{1}_{apf,Nf-1} & \vec{I}^{1}_{apf,Nf} \\ \vec{I}^{2}_{apf,1} & \vec{I}^{2}_{apf,2} & \cdots & \cdots & \vec{I}^{2}_{apf,Nf-1} & \vec{I}^{2}_{apf,Nf} \\ \vdots & \vdots & \vdots & \vdots & \vdots & \vdots \\ \vdots & \vdots & \vdots & \vdots & \vdots & \vdots \\ \vec{I}^{Nsa-1}_{apf,1} & \vec{I}^{Nsa-1}_{apf,2} & \cdots & \cdots & \vec{I}^{Nsa-1}_{apf,Nf-1} & \vec{I}^{Nsa-1}_{apf,Nf} \\ \vec{I}^{Nsa}_{apf,1} & \vec{I}^{Nsa}_{apf,2} & \cdots & \cdots & \vec{I}^{Nsa}_{apf,Nf-1} & \vec{I}^{Nsa}_{apf,Nf} \end{bmatrix} \tag{14}$$

Step-(3) Evaluation of the objective function: In this level, the fitness value for all search agents is determined using (11)

$$Fitness(t) = [Fitn_1, Fitn_2, \cdots, Fitn_{Nsa-1}, Fitn_{Nsa}]^T \tag{15}$$

Step-(4) Identification: The fitness values of above matrix (15) is sorted from lowest to highest and the first best solution is saved as alpha score and second and third best solutions are as beta score and delta score respectively. According to the scores, positions are also saved. The saved scores and positions are represented as

$$\vec{I}_{apf,\alpha,score}(t),\ \vec{I}_{apf,\beta,score}(t),\ \vec{I}_{apf,\delta,score}(t) \tag{16}$$

$$\vec{I}_{apf,\alpha,pos}(t),\ \vec{I}_{apf,\beta,pos}(t),\ \vec{I}_{apf,\delta,pos}(t) \tag{17}$$

Step-(5) Update the scores and positions of alpha, beta, and delta: In this step, the obtained scores and positions are related with the earlier scores at *(t-1)* *th* iteration of alpha, beta, and delta and the smallest value is stored as the new updated value. Correspondingly, the position is also updated.

$$\vec{I}_{apf,\alpha,score}(t) = \begin{Bmatrix} \vec{I}_{apf,\alpha,score}(t-1), & if\ \vec{I}_{apf,\alpha,score}(t) > \vec{I}_{apf,\alpha,score}(t-1) \\ \vec{I}_{apf,\alpha,score}(t), & if\ \vec{I}_{apf,\alpha,score}(t) \le \vec{I}_{apf,\alpha,score}(t-1) \end{Bmatrix} \tag{18}$$

Similarly, during $(t+1)^{th}$ iteration

$$\vec{I}_{apf,\alpha,score}(t+1) = \begin{Bmatrix} \vec{I}_{apf,\alpha,score}(t), & if\ \vec{I}_{apf,\alpha,score}(t+1) > \vec{I}_{apf,\alpha,score}(t) \\ \vec{I}_{apf,\alpha,score}(t+1), & if\ \vec{I}_{apf,\alpha,score}(t+1) \le \vec{I}_{apf,\alpha,score}(t) \end{Bmatrix} \tag{19}$$

Same way, scores and positions of beta and delta are also updated.

Step-(6) Update the position of search agents: In this action, using the encircling, hunting and attacking the prey concepts, the distance and position of $(ij)^{th}$ element is refreshed according to the position of alpha as

$$\vec{D}_{\alpha,ij} = |\vec{C}_{\alpha,ij} * \vec{I}_{apf,\alpha,pos,j}(t) - \vec{I}_{apf,pos,ij}(t)| \tag{20}$$

$$\vec{X}_{\alpha,ij} = \vec{I}_{apf,\alpha,pos,j}(t) - \vec{K}_{\alpha,ij} * \vec{D}_{\alpha,ij} \tag{21}$$

$$\vec{k}(t) = 2 - t*(2/T) \tag{22}$$

$$\vec{K}_{\alpha,ij} = 2*\vec{k}(t)*\vec{r}_1\alpha_{,ij} - \vec{k}(t) \tag{23}$$

$$\vec{C}_{\alpha,ij} = 2*\vec{r}_{2\alpha,ij} \tag{24}$$

where $i = 1,2,\ldots,\ldots,Nsa-1,Nsa;\ j = 1,2,\ldots,\ldots,Nf-1,Nf;$ Here, i and j denotes the row and column of matrix (14) respectively, t represents the current iteration, $\vec{r}_{1\alpha,ij}$ and $\vec{r}_{2\alpha}$, ij are the random vectors in (0,1) utilized to refresh the value of $(ij)^{th}$ elements of position matrix in terms of alpha, $\vec{K}_{\alpha,ij}$ and $\vec{C}_{\alpha,ij}$ are the coefficients vectors in terms of alpha.

It is worth noting here that, the authors of [43] have claimed that mathematical model of GWO is novel. It permits relocating a solution around another in an n-dimensional search space to simulate the natural behavior - chasing and encircling preys of grey wolves. So, the GWO estimates the global optimum compared to other algorithms. To avoid local optima avoidance and achieve global optima, GWO applies powerful operations controlled by its parameters to maintain the

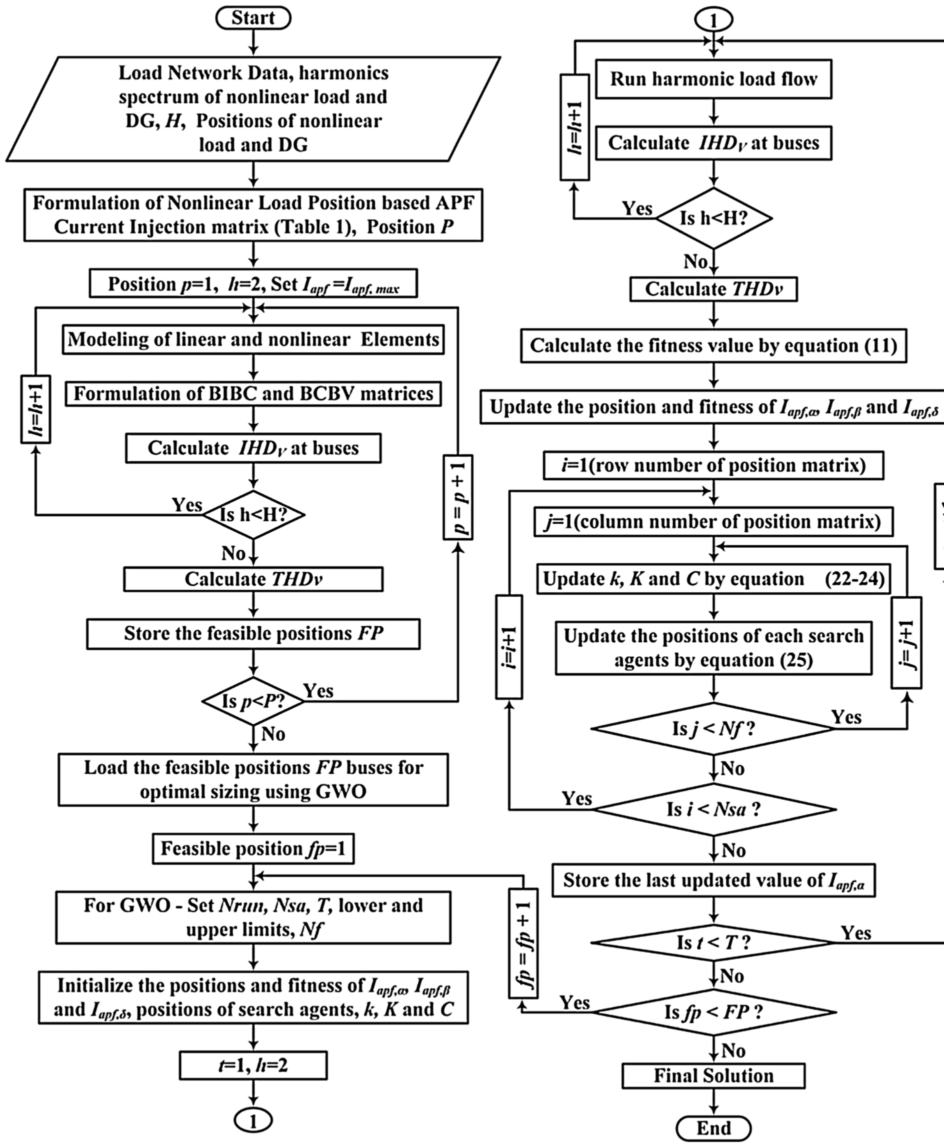

Fig. 3. Flowchart for NLPCI plus GWO for OPAS of multiple APFs in RDS for nonlinear loads and NLDGs.

balance between exploration and exploitation phases. The $\vec{C}_{\alpha,ij}$ and $\vec{K}_{\alpha,ij}$ performs their role in exploration phase and $\vec{k}$ in exploitation phase. The $\vec{C}_{\alpha,ij}$ has always a random value in the interval of [0,2]. Due to this randomization the prey takes the new position. When $\vec{C}_{\alpha,ij} > 1$, the solution inclines more towards the prey. This parameter has random value therefore; exploration is emphasized during optimization in case of any local optima immobility. The value of $\vec{K}_{\alpha,ij}$ depends on the value of $\vec{k}$, which is linearly decreases from 2 to 0. It has also random components therefore; parameter $\vec{K}_{\alpha,ij}$ has value in between -2 to 2. When $\vec{K}_{\alpha,ij} > 1$, or $\vec{K}_{\alpha,ij} < -1$ the exploration is promoted, while $\vec{K}_{\alpha,ij}$ has value $-1 < \vec{K}_{\alpha,ij} < 1$, it highlights the exploitation. The good balance is required in exploration phase and exploitation phase to find the global optima using stochastic behavior of algorithm. It is achieved in the GWO, by decreasing nature of the $\vec{k}$ in the equation of $\vec{K}_{\alpha,ij}$.

The distance and positions of beta and delta are renewed as alpha. The distance and position of *(ij)*th element is updated according to the position of alpha, beta, and delta and given as

$$\vec{I}^{\,i}_{apf,j}(t+1) = \frac{\vec{X}_{\alpha,ij} + \vec{X}_{\beta,ij} + \vec{X}_{\delta,ij}}{3} \quad (25)$$

Step-(7) Update the elements: Update the value of all elements of the position matrix using (25)

Step-(8) Repeat steps (3–7) up to maximum iterations (T).

The updated value of $\vec{I}_{apf,\alpha,score}$ after Tth iteration is the optimum value of APF current and corresponding position is individual filter current $\vec{I}_{apf,\alpha,pos}$. The NLPCI technique is described in the next section.

3. NLPCI technique

It is used to find the feasible buses among all 33 buses. Fig. 4 shows the 33-bus system under consideration with the possible location of APFs [44]. Here, it is assumed that the constant nonlinear loads are connected at 18, 22, 25 and 33 buses with the same harmonics spectrum as shown in Fig. 5. It is 5th to 49th order of harmonics.

It is to be understood that the APFs are to be connected to the buses 18, 22, 25, and 33. Without using GWO and NLPCI the numbers of APFs, as well as ratings, would be higher. Here, NLPCI is used to identify the feasible buses, and GWO is used to obtain the least possible rating of the APFs considering 5% THDv limits. It means that not going for 0% THDv (that is also possible with connecting the APFs at all nonlinear load buses) but to exploit (going for 4.8 or 4.9% THDv is fine)

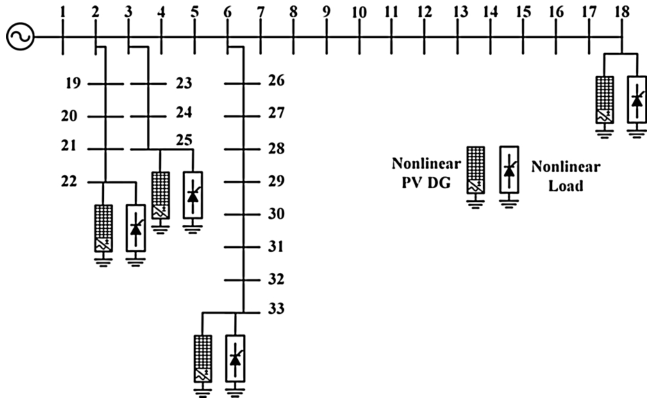

Fig. 4. 33-bus RDS with nonlinear loads and NLDGs.

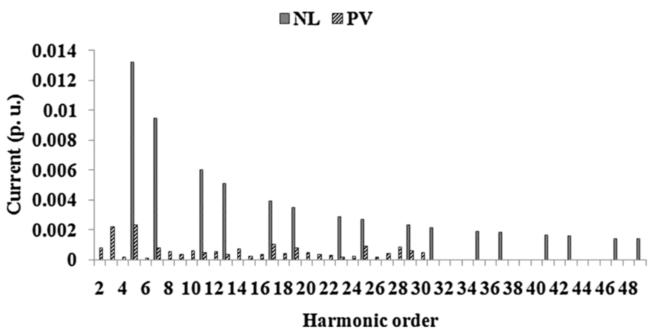

Fig. 5. Harmonic spectrum of nonlinear load and nonlinear PV.

Table 1
APFs at various buses considered in NLPCI.

State/APF Bus	No. of APFs	Bus no. 18	Bus no. 22	Bus no. 25	Bus no. 33
P_1	One	1	0	0	0
P_2		0	1	0	0
P_3		0	0	1	0
P_4		0	0	0	1
P_5	Two	1	1	0	0
P_6		1	0	1	0
P_7		1	0	0	1
P_8		0	1	1	0
P_9		0	1	0	1
P_{10}		0	0	1	1
P_{11}	Three	1	1	1	0
P_{12}		1	0	1	1
P_{13}		1	1	0	1
P_{14}		0	1	1	1
P_{15}	Four	1	1	1	1

the IEEE standard of 5% is practicable and cost-effective. Although, GWO can perform both these tasks that is to find out OPAS of APFs to be connected in RDS with the NLDGs and nonlinear loads, yet the task of finding out the location can be performed faster and with least complexity by NLPCI. Hence, NLPCI is reducing the burden on GWO. Table 1 presents the possible combination of numbers of APFs as per the position of the nonlinear loads and NLDGs. In this, '1' indicates the presence of APF and '0' indicates absence of APF. These combinations can be 1 or 2 or 3 or 4 APFs connected at a time with the given 33 bus system. Here, the judgment of the feasible bus(es) once taken from the Table 1, APFs having the same rating as that of the nonlinear load is to be connected, and thus by doing this exercise, the THDv is checked for the allowable limits.

Table 3
Feasibility table according to NLPCI.

Position of APF	Feasibility	Maximum THDv and its bus number		Bus number at APF placed	Numbers of APF	Total current rating of APF (p.u.)
P_1	No	9.45	33	18	One	0.019747
P_2	No	19.50	18	22	One	0.019747
P_3	No	19.09	18	25	One	0.019747
P_4	No	17.29	18	33	One	0.019747
P_5	No	9.37	33	18,22	Two	0.039494
P_6	No	8.95	33	18,25	Two	0.039494
$\mathbf{P_7}$	**Yes**	**4.97**	**22**	**18,33**	**Two**	**0.039494**
P_8	No	19.01	18	22,25	Two	0.039494
P_9	No	17.21	18	22,33	Two	0.039494
P_{10}	No	16.80	18	25,33	Two	0.039494
P_{11}	No	8.87	33	18,22,25	Three	0.059241
$\mathbf{P_{12}}$	**Yes**	**4.90**	**22**	**18,25,33**	**Three**	**0.059241**
$\mathbf{P_{13}}$	**Yes**	**3.33**	**25**	**18,22,33**	**Three**	**0.059241**
P_{14}	No	16.72	18	22,25,33	Three	0.059241
$\mathbf{P_{15}}$	**Yes**	**0.00**	**nil**	**18,22,25,33**	**Four**	**0.078988**

The feasible positions are highlighted in bold.

4. Results and discussion

In this section, the results are obtained using NLPCI and optimization algorithms and discussed in detailed.

4.1. Case 1: nonlinear load

In this case, only nonlinear load is considered.

Table 2 shows the results for THDv (%) at different buses in the absence of APFs. It is clear from that the violation of THDv limit is observed at the various buses. Among the 33 buses, 22 buses have THDv more than the allowable limit. Hence, filters are necessary at the selected buses to obtain the THDv within the specified limits at all the buses. Table 3 shows the possible solutions available from Table 1 for the placement, numbers of APFs, size of APFs and maximum THDv percentage with the bus number. Thus, Table 3 is a solution according to NLPCI. It is clear that the position of APFs are at P_7 (two APFs at bus numbers 18 and 33), P_{12} (three APFs at bus numbers 18, 25 and 33), P_{13} (three APFs at bus numbers 18, 22 and 33), P_{15} (four APFs at bus numbers 18, 22, 25 and 33) are feasible states. Here, the rating of the

Table 2
THDv (%) at different buses with nonlinear loads without APFs.

Bus Number	THDv (%)	Bus Number	THDv (%)	Bus Number	THDv (%)	Bus Number	THDv (%)
2	0.31	**10**	**10.65**	**18**	**19.58**	**26**	**5.32**
3	1.56	**11**	**10.76**	19	0.57	**27**	**5.56**
4	2.18	**12**	**10.96**	20	2.80	**28**	**7.10**
5	2.83	**13**	**12.87**	21	3.59	**29**	**8.26**
6	**5.15**	**14**	**14.04**	**22**	**5.13**	**30**	**8.69**
7	**6.17**	**15**	**14.91**	23	2.07	**31**	**10.27**
8	**8.20**	**16**	**15.81**	24	3.24	**32**	**10.87**
9	**9.43**	**17**	**18.63**	25	4.40	**33**	**11.74**

The buses have THDv more than 5% are highlighted in bold.

Table 4
Comparative value of APF current by different methods and algorithms for APF considering nonlinear load.

Sr. No.	Position of APFs with APFs	APF current (p.u.)						Total cost of APFs ($)
		Without optimization	With NLPCI	GWO	PSO	HS	% of APF current by GWO compared to without optimization	
1	P_7 (2)	0.078988	0.039494	0.033022	0.033058	0.033061	41.81	203,776
2	P_{12} (3)	0.078988	0.059241	0.033026	0.034571	0.034482	41.81	293,779
3	P_{13} (3)	0.078988	0.059241	0.026860	0.033557	0.059889	34.01	289,339
4	P_{15} (4)	0.078988	0.078988	0.027136	29.548769	57.977526	34.35	379,538

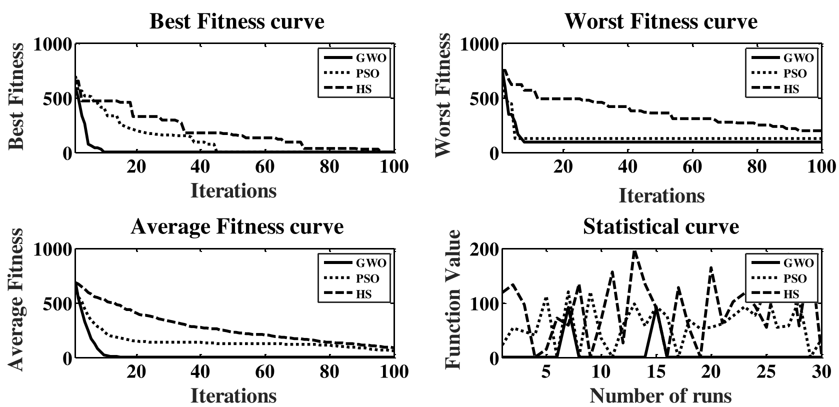

Fig. 6. Computational tests for GWO, PSO, and HS for finding the optimal size of APFs at 18, 22 and 33 buses.

Table 5
THDv (%) at different buses in the absence of filter for nonlinear load and NLDG.

Bus number	THDv (%)	Bus number	THDv (%)	Bus number	THDv (%)	Bus number	THDv (%)
2	0.35	**10**	**11.80**	**18**	**21.69**	**26**	**5.90**
3	1.73	**11**	**11.92**	19	0.63	**27**	**6.17**
4	2.42	**12**	**12.15**	20	3.10	**28**	**7.87**
5	3.13	**13**	**14.26**	21	3.98	**29**	**9.15**
6	**5.71**	**14**	**15.56**	**22**	**5.68**	**30**	**9.62**
7	**6.83**	**15**	**16.52**	23	2.30	**31**	**11.38**
8	**9.09**	**16**	**17.51**	24	3.59	**32**	**12.04**
9	**10.44**	**17**	**20.64**	25	4.87	**33**	**13.00**

The buses have THDv more than 5% are highlighted in bold.

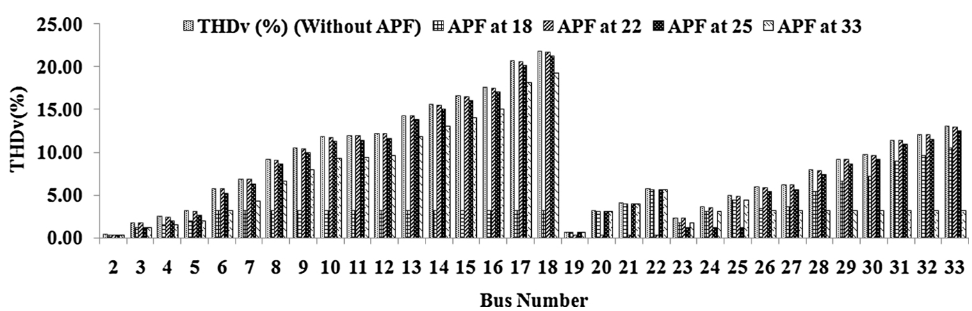

Fig. 7. Voltage conditions at different buses after applying one APF at different buses for nonlinear loads and NLDGs.

nonlinear loads and rating of the APFs are same. Therefore, the sizes of APFs are high. It is very costly. To reduce the size means the cost of APF, GWO is implemented. With the application of GWO, the rating of these APFs can be reduced by a great deal and thus the optimization is achieved (size optimization).

The comparative results for different techniques and optimization algorithms are tabulated in Table 4. It demonstrates the importance of optimal placement. The required current of APFs found by GWO is the lowest among all considered optimization algorithms. The GWO found the lowest results for two APFs, three APFs (both cases) and four APFs. It shows the stability of GWO such that in all cases it found the optimal results. By using NLPCI plus GWO OPAS of APFs is found. The lowest current found by GWO is only 34% of unoptimized solution for three filters at buses 18, 22 and 33 while it is 41.81% in case of APFs are at 18, 25 and 33. If only the current is a criteria then best solution is APFs are placed at P_{13}, but it is with three filters, a costly solution.

The realistic investment cost of APF is divided into two parts: (1) Constant cost (installation cost, it depends only on the number of APF) and (2) Incremental cost (it proportional to APF current). In this paper installation cost is considered and added to incremental cost. Here, NLPCI finds the feasible buses, means number of APFs (installation cost) and GWO finds the minimum current of APF (incremental cost).

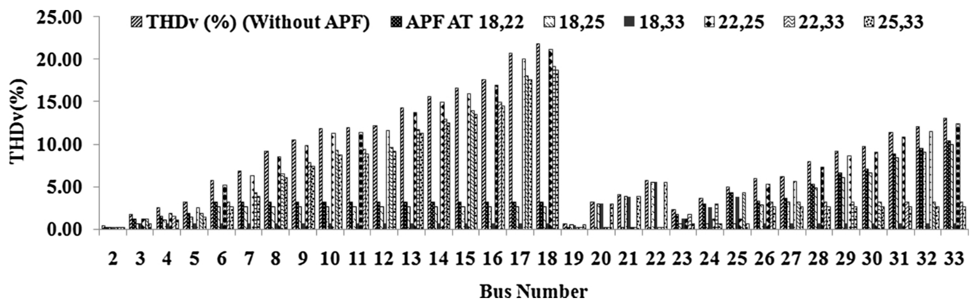

Fig. 8. Voltage conditions at different buses after applying two APFs for nonlinear loads and NLDGs.

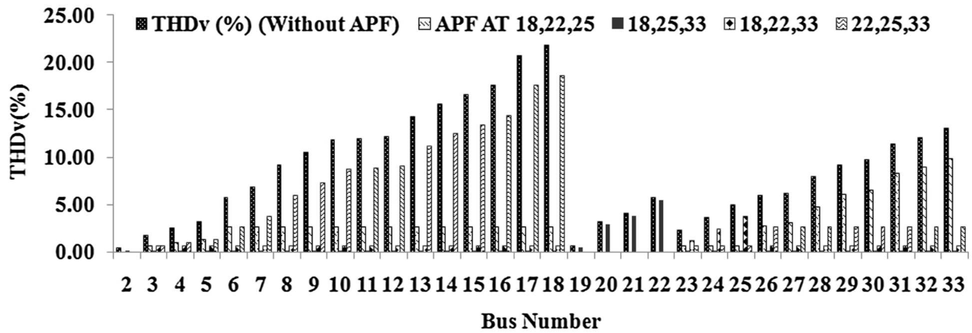

Fig. 9. Voltage conditions at different buses after applying three APFs for nonlinear loads and NLDGs.

Based on [29], the fixed cost of an AFP is taken as 90,000$ and incremental cost of an APF is taken as 720,000$ per p.u. of APF current. The last column of Table 4 presents the cost of APF. It is clear that minimum current of APF is for three APFs at buses 18, 22 and 23, but cost is high due to number of APFs are more compared to APFs at buses at 18 and 33. It shows the importance of installation cost in cost calculation. The cost for two APFs is lowest compared to all other solutions. It is 49% only compared to cost of unoptimized solution (416,871$).

Fig. 6 shows the computational tests- best value, worst value, an average value and statistical curve for GWO, PSO, and HS. The tests are performed with 40 search agents and 100 iterations for 30 runs. From this figure, it is found that the GWO has outperformed the other considered algorithms. The GWO has the best value (0.026860 p.u.) and converged fast compared to different algorithms. As the iterations are increasing the average value is decreasing. The GWO has the lowest average value with the highest rate of convergence. From the statistical test, it is observed that the curve of GWO is smooth. It has fewer spikes compared to other algorithms. It means that the GWO is consistent and highly stable. Moreover, GWO has the lowest value of worst fitness compared to PSO and HS. The solution found by GWO is minimum. The PSO and HS could not attain the optimum solution that GWO could. It shows the significant outcomes compared to PSO and HS for considered OPAS of APF problem by performing better than PSO and HS in all computational tests.

4.2. Case 2: nonlinear loads plus NLDGs

The case presented above was with nonlinear loads only. Now, the nonlinear loads with the NLDGs (Solar PV generators) are also considered for the analysis. It is assumed that all NLDG has the same harmonic spectrum as shown in Fig. 5 [45]. It is differing than nonlinear load, it is 2^{nd} to 30^{th} order of harmonics. They are connected at all nonlinear load buses. The complete study is shown in Table 5 (without APF), Fig. 7 (with 1 APF only at the different buses), Fig. 8 (with 2 APFs at the different buses), and Fig. 9 (with 3 APFs at the different buses). The results are very much identical apart from the two cases viz. when two APFs were used in the various combinations, the feasible solution was not available (all the instances give THDv higher than 5%) and when three APFs are used the only viable solution is at the bus numbers 18,22, and 33.

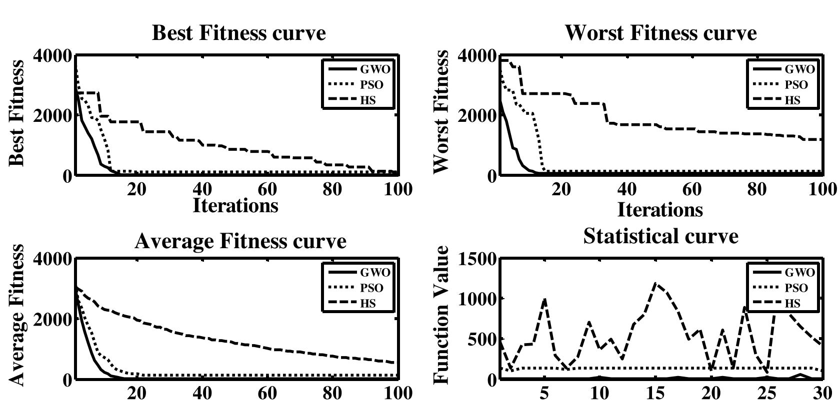

Fig. 10. Computational tests for GWO, PSO and HS for finding the optimal size of APFs at 18, 22 and 33 buses.

Table 6
Comparative value of APF current by different methods and algorithms considering nonlinear load plus DG.

Sr. No.	Position of APFs with APFs	APF current (p.u.)						Total cost of APFs ($)
		Without optimization	With NLPCI	GWO	PSO	HS	%of APF current by GWO compared to without optimization	
1	P_{13} (3)	0.090358	0.067769	0.033906	101.047019	82.770849	37.52	294,412
2	P_{15} (4)	0.090358	0.090358	0.034211	134.46	427.6	37.86	384,632

Table 7
Summary statistics for nonlinear load, NLDG, and nonlinear load plus NLDG.

Case	Max. THDv (%)	Buses more than 5% THDv	Number of APF required	Total rating of APF (p.u.)	% APF size compared with without optimization
Only nonlinear load	19.58	22	2	0.033022	41.81
			3	0.026860	34.01
Only NLDG	3.92	Nil	Nil	Nil	Nil
Nonlinear load plus NLDG	21.69	22	3	0.033906	37.52
Change in Nos. of APF and size due to NLDG			1	2.67 % increased	
			Nil	26.23 % increased	

4.3. Results with NLPCI- one APF, two APFs and three APFs

Table 6 presents a comparative analysis of the value of APF current by different methods and algorithms for APF considering nonlinear load plus NLDGs. The Table 6 and the associated Figs. 7–10 are enough to prove that again the results of NLPCI plus GWO are compared with the PSO and HS algorithms, and it is found that NLPCI plus GWO gives better results than PSO or HS algorithms. The APF current is minimized for NLPCI plus GWO and computational tests considering best fitness, worst fitness, average fitness and the statistical values are much better for concerning the other two algorithms. This again proves the adaptability of NLPCI plus GWO method. The cost of optimal solution is 294,412$, which is only the 69% of cost of unoptimized solution (425,058$).

Table 7 summarized the results of all cases. It is interesting that only NLDG is considered the constraints are fulfilled, no requirement of APF/APFs, and while in case of a nonlinear load plus NLDG the required APFs are increased from two to three. Finally, due to NLDG, one more APF with an increased rating of 2.67% or with three APFs increased rating of 26.23% are placed to mitigate the harmonics up to the standard limit. It is substantial evidence of the effect of NLDG on OPAS of APF in RDS.

5. Conclusion

The paper has proposed the new technique NLPCI system to locate the ideal position of APF for two cases (1) with inclusion of nonlinear loads only and (2) with inclusion of nonlinear loads along with NLDG. The GWO is used to recognize the optimal size of APF. The size of APF is more prominent for the nonlinear load combined with the NLDG in comparison to the nonlinear loads only. NLPCI is validated through the GWO, PSO and HS algorithms by comparing feasible and infeasible positions of APF considering different buses. The results of GWO are compared with the PSO and HS algorithms, and it is found that GWO gives better results than PSO and HS algorithms. The APF current is minimized for GWO and computational tests considering best fitness, worst fitness, average fitness and the statistical values are much better for concerning the other two algorithms. THDv limit of 5% is exploited to save the size of APF with the proposed method. The analysis shows that the % current of APF current by GWO compared to that without optimization is much smaller. The optimization has reduced the APF ratings by nearly 2.5 times.

References

[1] T. Ackermann, G. Andersson, L. Söder, Distributed generation: a definition1, Electr. Power Syst. Res. 57 (2001) 195–204.
[2] U. Sultana, A.B. Khairuddin, A. Mokhtar, N. Zareen, B. Sultana, Grey wolf optimizer based placement and sizing of multiple distributed generation in the distribution system, Energy 111 (2016) 525–536.
[3] C.L. Borges, D.M. Falcao, Optimal distributed generation allocation for reliability, losses, and voltage improvement, Int. J. Electr. Power Energy Syst. 28 (2006) 413–420.
[4] G. Bruni, S. Cordiner, V. Mulone, Domestic distributed power generation: effect of sizing and energy management strategy on the environmental efficiency of a photovoltaic-battery-fuel cell system, Energy Oxf. (Oxf.) 77 (2014) 133–143.
[5] R. Walling, R. Saint, R.C. Dugan, J. Burke, L.A. Kojovic, Summary of distributed resources impact on power delivery systems, IEEE Trans. Power Delivery 23 (2008) 1636–1644.
[6] F. Guan, D. Zhao, X. Zhang, B. Shan, Z. Liu, Research on distributed generation technologies and its impacts on power system, Sustainable Power Generation and Supply, 2009. SUPERGEN'09. International Conference on, IEEE, (2009), pp. 1–6.
[7] M.H. Bollen, R. Das, S. Djokic, P. Ciufo, J. Meyer, S.K. Rönnberg, F. Zavodam, Power quality concerns in implementing smart distribution-grid applications, IEEE Trans. Smart Grid 8 (2017) 391–399.
[8] F. Wang, J.L. Duarte, M.A. Hendrix, P.F. Ribeiro, Modeling and analysis of grid harmonic distortion impact of aggregated DG inverters, IEEE Trans. Power Electron. 26 (2011) 786–797.
[9] V. Hengsritawat, T. Tayjasanant, N. Nimpitiwan, Optimal sizing of photovoltaic distributed generators in a distribution system with consideration of solar radiation and harmonic distortion, Int. J. Electr. Power Energy Syst. 39 (2012) 36–47.
[10] J.H. Enslin, P.J. Heskes, Harmonic interaction between a large number of distributed Power inverters and the distribution network, IEEE Trans. Power Electron. 19 (2004) 1586–1593.
[11] M.P. HA, P.D. Huy, V.K. Ramachandaramurthy, A review of the optimal allocation of distributed generation: objectives, constraints, methods, and algorithms, Renewable Sustain. Energy Rev. 75 (2017) 293–312.
[12] S. Sakar, M.E. Balci, S.H.A. Aleem, A.F. Zobaa, Increasing PV hosting capacity in distorted distribution systems using passive harmonic filtering, Electr. Power Syst. Res. 148 (2017) 74–86.
[13] S. Sakar, M.E. Balci, S.H.A. Aleem, A.F. Zobaa, Integration of large-scale PV plants in non-sinusoidal environments: Considerations on hosting capacity and harmonic distortion limits, Renewable Sustain. Energy Rev. 82 (2018) 176–186.
[14] V.R. Pandi, H. Zeineldin, W. Xiao, A.F. Zobaa, Optimal penetration levels for inverter-based distributed generation considering harmonic limits, Electr. Power Syst. Res. 97 (2013) 68–75.
[15] P.G. Khorasani, M. Joorabian, S.G. Seifossadat, Smart grid realization with introducing unified power quality conditioner integrated with DC microgrid, Electr. Power Syst. Res. 151 (2017) 68–85.
[16] N. Kumar, A. Kumar, Techno-economic analysis of non-linear DG penetration in radial distribution systems, Distrib. Gener. Altern. Energy J. 32 (2017) 54–74.
[17] IEEE Recommended Practice and Requirements for Harmonic Control in Electric Power Systems, IEEE, New York, NY, 2014.
[18] B. Singh, K. Al-Haddad, A. Chandra, A review of active filters for power quality improvement, IEEE Trans. Ind. Electron. 46 (1999) 960–971.
[19] M. Gomez-Gonzalez, A. López, F. Jurado, Optimization of distributed generation systems using a new discrete PSO and OPF, Electr. Power Syst. Res. 84 (2012)

174–180.
[20] A. Pagnetti, G. Delille, A simple and efficient method for fast analysis of renewable generation connection to active distribution networks, Electr. Power Syst. Res. 125 (2015) 133–140.
[21] T. Soares, F. Pereira, H. Morais, Z. Vale, Cost allocation model for distribution networks considering high penetration of distributed energy resources, Electr. Power Syst. Res. 124 (2015) 120–132.
[22] V. Murty, A. Kumar, Optimal placement of DG in radial distribution systems based on new voltage stability index under load growth, Int. J. Electr. Power Energy Syst. 69 (2015) 246–256.
[23] A. Uniyal, A. Kumar, Optimal distributed generation placement with multiple objectives considering probabilistic load, Procedia Comput. Sci. 125 (2018) 382–388.
[24] H. Liao, J.V. Milanović, Techno-economic analysis of global power quality mitigation strategy for provision of differentiated quality of supply, Int. J. Electr. Power Energy Syst. 107 (2019) 159–166.
[25] S.M. Ismael, S.H.A. Aleem, A.Y. Abdelaziz, A.F. Zobaa, State-of-the-art of hosting capacity in modern power systems with distributed generation, Renew. Energy (2018).
[26] R. Keypour, H. Seifi, A. Yazdian-Varjani, Genetic based algorithm for active power filter allocation and sizing, Electr. Power Syst. Res. 71 (2004) 41–49.
[27] I. Ziari, A. Jalilian, A new approach for allocation and sizing of multiple active power-line conditioners, IEEE Trans. Power Delivery 25 (2010) 1026–1035.
[28] I. Ziari, A. Jalilian, Optimal allocation and sizing of active power line conditioners using a new particle swarm optimization-based approach, Electr. Power Compon. Syst. 40 (2012) 273–291.
[29] I. Ziari, A. Jalilian, Optimal placement and sizing of multiple APLCs using a modified discrete PSO, Int. J. Electr. Power Energy Syst. 43 (2012) 630–639.
[30] J. Kennedy, R.C. Eberhart, Particle swarm optimization, Proceedings of IEEE International Conference on Neural Networks (1995) 1942–1948.
[31] F.M. Alhaddad, Optimal Filter Placement and Sizing Using Ant Colony Optimization in Electrical Distribution System, (2014).
[32] Z.W. Geem, J.H. Kim, G. Loganathan, A new heuristic optimization algorithm: harmony search, Simulation 76 (2001) 60–68.
[33] M. Shivaie, A. Salemnia, M.T. Ameli, Optimal multi-objective placement and sizing of passive and active power filters by a fuzzy-improved harmony search algorithm, Int. Trans. Electr. Energy Syst. (2013).
[34] M. Shivaie, A. Salemnia, M.T. Ameli, A multi-objective approach to optimal placement and sizing of multiple active power filters using a music-inspired algorithm, Appl. Soft Comput. 22 (2014) 189–204.
[35] M. Farhoodnea, A. Mohamed, H. Shareef, H. Zayandehroodi, Optimum placement of active power conditioners by a dynamic discrete firefly algorithm to mitigate the negative power quality effects of renewable energy-based generators, Int. J. Electr. Power Energy Syst. 61 (2014) 305–317.
[36] M. Moghbel, M.A. Masoum, A. Fereidouni, S. Deilami, Optimal sizing, siting and operation of custom power devices with STATCOM and APLC functions for real-time reactive power and network voltage quality control of smart grid, IEEE Trans. Smart Grid 9 (2018) 5564–5575.
[37] D.H. Wolpert, W.G. Macready, No free lunch theorems for optimization, IEEE Trans. Evol. Comput. 1 (1997) 67–82.
[38] J.-H. Teng, S.-H. Liao, R.-C. Leou, Three-phase harmonic analysis method for unbalanced distribution systems, Energies 7 (2014) 365–384.
[39] Z. Michalewicz, A survey of constraint handling techniques in evolutionary computation methods, Evol. Program. 4 (1995) 135–155.
[40] S. Mirjalili, S.M. Mirjalili, A. Lewis, Grey wolf optimizer, Adv. Eng. Softw. 69 (2014) 46–61.
[41] M. Shakarami, I.F. Davoudkhani, Wide-area power system stabilizer design based on grey wolf optimization algorithm considering the time delay, Electr. Power Syst. Res. 133 (2016) 149–159.
[42] C. Castillo, A. Conde, E. Fernandez, Mitigation of DOCR miscoordination through distance relays and non-standard overcurrent curves, Electr. Power Syst. Res. 163 (2018) 242–251.
[43] H. Faris, I. Aljarah, M.A. Al-Betar, S. Mirjalili, Grey wolf optimizer: a review of recent variants and applications, Neural Comput. Appl. (2018) 1–23.
[44] S.A. Taher, M. Hasani, A. Karimian, A novel method for optimal capacitor placement and sizing in distribution systems with nonlinear loads and DG using GA, Commun. Nonlinear Sci. Numer. Simul. 16 (2011) 851–862.
[45] A.R. Oliva, J.C. Balda, A PV dispersed generator: a power quality analysis within the IEEE 519, IEEE Trans. Power Delivery 18 (2003) 525–530.